

Probing Neutrino Dirac Mass in Left-Right Symmetric Models at the LHC and Next Generation Colliders

Juan Carlos Helo^{1*}, Haolin Li^{2,6†}, Nicolás A. Neill^{3,4‡},
Michael Ramsey-Musolf^{2,5§} and Juan Carlos Vasquez^{3,4⊗}

Departamento de Física, Facultad de Ciencias, Universidad de La Serena,
La Serena, Chile¹

Amherst Center for Fundamental Interactions, Department of Physics,
University of Massachusetts-Amherst, U.S.A²

Departamento de Física Universidad Técnica Federico Santa María,
Valparaíso, Chile³

Centro Científico Tecnológico de Valparaíso, Valparaíso, Chile⁴
Kellogg Radiation Laboratory, California Institute of Technology,

Pasadena, CA 91125 USA⁵

Institute of Theoretical Physics, China Academic of Science,
Beijing 100190, China⁶

E-mail: jchelo@userena.cl^{*}, lihaolin1991@gmail.com[†], mjrm@physics.umass.edu[§],
nicolas.neill@gmail.com[‡], juan.vasquezcar@usm.cl[⊗]

We assess the sensitivity of the LHC, its high energy upgrade, and a prospective 100 TeV hadronic collider to the Dirac Yukawa coupling of the heavy neutrinos in left-right symmetric models (LRSMs). We focus specifically on the trilepton final state in regions of parameter space yielding prompt decays of the right-handed gauge bosons (W_R) and neutrinos (N_R). In the minimal LRSM, the Dirac Yukawa couplings are completely fixed in terms of the mass matrices for the heavy and light neutrinos. In this case, the trilepton signal provides a direct probe of the Dirac mass term for a fixed W_R and N_R mass. We find that while it is possible to discover the W_R at the LHC, probing the Dirac Yukawa couplings will require a 100 TeV pp collider. We also show that the observation of the trilepton signal at the LHC would indicate the presence of a non-minimal LRSM scenario.

1 Introduction

Soon after the appearance of the original works [1–3], the minimal left-right symmetric model (mLRSM) has been proposed to connect the smallness of neutrino masses with the spontaneous violation of parity [4–6]. The origin of neutrino masses within the mLRSM must be understood in analogy with the explanation of the origin of mass within the Standard Model (SM). In the SM, fermion masses are obtained through the Higgs mechanism, for which one manifestation is the proportionality of a given Higgs boson fermionic branching ratio to the square of the corresponding fermion mass. The Higgs boson has been discovered at the LHC by the ATLAS and CMS collaborations [7], and the measured branching ratio into bottom quark and τ lepton pairs agree with the SM expectations [8].

In the neutrino sector, the situation becomes less clear since neutrinos are electrically neutral. While an SM-like pure Dirac mass is a possibility, the magnitudes of associated Yukawa couplings would be considerably smaller than for the charged elementary fermions. A theoretically attractive alternative is the see-saw mechanism [5, 9–13], which exploits the possibility that the electrically neutral neutrino may be its own antiparticle. Neutrino masses in the mLRSM arise from a combination of two versions of the see-saw mechanism, the so-called Type-I, and Type-II variants.

If left-right symmetry is realized in nature, it will be important to establish whether the mLRSM is at the same level as the SM regarding the origin of fermion masses. Soon after its original proposal, approaches for probing the Yukawa couplings of heavy and light neutrinos were considered. The Yukawa sector for the light neutrinos may be in principle probed in low energy experiments, such as neutrinoless double beta decay and oscillation experiments. The Yukawa couplings of heavy neutrinos (HNs) can be probed in high energy experiments through the Keung-Senjanović (KS) process [14], which consists in the production of an on-shell, heavy W_R gauge boson decaying into two right-handed leptons and two jets. More recently, in Refs. [15–17] it was found that the Dirac Yukawa coupling of neutrinos (which is proportional to the mixing between heavy and light neutrinos) can be unambiguously obtained once all light and heavy neutrino masses and mixing angles are measured. Therefore, this puts the mLRSM as a *testable* model of neutrino masses and calls for the experimental verification of the relation between the Dirac mass and the heavy and light neutrino masses, the main subject of this work.

It is worth emphasizing that without left-right symmetry, the connection between the Dirac mass matrix and the heavy and light neutrino mass matrices is lost. This can be explicitly seen in the Casas-Ibarra parametrization [18], where the Dirac mass matrix is given in terms of the heavy and light neutrino mass matrices up to an arbitrary complex, orthogonal matrix, whose elements are not even bounded. This situation contrasts with the mLRSM, since within this

framework the imposition of a discrete LR symmetry is sufficient to fix the arbitrary orthogonal matrix in terms of the heavy and light neutrino mass matrices (see for instance Refs. [15–17]).

The Dirac Yukawa coupling of heavy neutrinos could in principle be probed by considering angular asymmetries in the channel with one right-handed charged lepton, one left-handed charged lepton and two jets in the final state [15]. In practice, as we shall show, this may not be feasible with the statistics one expects even at the 100 TeV machine. The reason is that for a large number of events N , the statistical error goes as \sqrt{N} and hence the asymmetry one wishes to measure should be at least of the order of $\sqrt{N}/N = 1/\sqrt{N}$. For instance, for the mLRSM and in the best case scenario with W_R boson mass of 6 TeV, the branching ratio of the HNs to charge leptons and one W boson is of the order of 10^{-4} . Hence, probing this small branching ratio would require at least 10^8 signal events, which is not feasible at either the LHC with high luminosity or a next 100 TeV pp -collider. For a complete phenomenological study of the two leptons and two jets channel, see *e.g.* Refs. [19, 20].

Consequently, in this work we propose instead that the ideal channel for probing the Dirac mass term of heavy neutrinos is through the purely leptonic decay $W_R^\pm \rightarrow l^\pm N \rightarrow l^\pm (N \rightarrow l'^\pm W^\mp \rightarrow l^\pm l'^\mp \nu)$. This channel has been previously studied in the context of the type I see-saw extension of the SM with fermion singlets in Ref. [21] and more recently searched for by the CMS collaboration [22]. It has also been studied in the context of a left-right symmetric model with an inverse see-saw mechanism in Ref. [23].

It provides a cleaner signal that has an advantage with respect to the KS channel since no asymmetry needs to be measured. Our main findings may be summarized as follows: in order to test the mLRSM prediction for the mixing between the heavy and light neutrinos (or equivalently the Dirac mass), one must consider a next generation collider beyond the LHC, such as a 100 TeV pp collider. On the other hand, and if one observes evidence for this mixing at the LHC, it would point to a non-minimal scenario within the context of LRSMs.

The discussion of our study leading to these findings is organized as follows. In Sec. 2, we briefly introduce the model in both its minimal and non-minimal incarnations. Assuming charge conjugation as the left-right symmetry for the minimal case, we explain the relationship between the Dirac mass matrix in terms of the heavy and light neutrino mass matrices. This connection is crucial to obtain the sensitivity to the Dirac mass. In Sec. 3, we estimate the sensitivity at the LHC, High Energy LHC (HE-LHC) and a 100 TeV pp collider to heavy-light neutrino mixing. We compare the reaches of these various colliders to the expectations within the mLRSM and non-minimal model discussed in Section 2. In Sec. 4 and within the minimal model, we translate the sensitivity to the heavy-light neutrino mixing into a reach on the Dirac mass. Finally in Sec. 5 the conclusions are given.

2 The left-right symmetric model

2.1 The minimal left-right symmetric model

The minimal left-right symmetric model [1–3] was introduced in order to explain the smallness of neutrino mass in connection with the spontaneous violation of Parity [4–6]. In this work we do not pursue the $\mathcal{O}(1)$ Yukawa couplings of neutrinos, that is, without special Yukawa texture [24–31] or cancellation between Type I and Type II see-saw effect [32–34]. In this case, the LR symmetry breaking scale would be very high, such that the W_R boson and heavy neutrino will be too heavy to be produced even in a future 100 TeV collider. Instead, we consider the minimal framework, where we have relatively small Yukawa couplings ($\mathcal{O}(10^{-6} \sim 10^{-5})$) with relatively light W_R boson mass ($\mathcal{O}(1 \sim 10)\text{TeV}$) and in the reach of present and future colliders.

The gauge group and field content: the gauge group is $\mathcal{G} = SU(2)_L \times SU(2)_R \times U(1)_{B-L}$, with an additional discrete symmetry that may be generalized parity (\mathcal{P}) or charge conjugation (\mathcal{C}). The quarks and leptons are doublets in the following irreducible representations of the gauge group:

$$\begin{aligned} q_L &= \begin{pmatrix} u \\ d \end{pmatrix}_L : (2, 1, \frac{1}{3}), & q_R &= \begin{pmatrix} u \\ d \end{pmatrix}_R : (1, 2, \frac{1}{3}), \\ L_L &= \begin{pmatrix} \nu \\ l \end{pmatrix}_L : (2, 1, -1), & L_R &= \begin{pmatrix} N \\ l \end{pmatrix}_R : (1, 2, -1). \end{aligned} \tag{1}$$

Where N represents the new heavy neutrino states, whose presence explain the smallness of neutrino masses on the basis of the see-saw mechanism [5, 9–13].

The Higgs sector of the mLRSM [5, 9], consists in one bidoublet Φ , in the (2,2,0) representation of \mathcal{G} and two scalar triplets Δ_L and Δ_R , belonging to (3,1,2) and (1,3,2) representation respectively

$$\Phi = \begin{pmatrix} \phi_1^0 & \phi_2^+ \\ \phi_1^- & \phi_2^0 \end{pmatrix}, \quad \Delta_{L,R} = \begin{pmatrix} \delta_{L,R}^+/\sqrt{2} & \delta_{L,R}^{++} \\ \delta_{L,R}^0 & -\delta_{L,R}^+/\sqrt{2} \end{pmatrix}. \tag{2}$$

After SSB, the v.e.v's of the Higgs fields may be written as [6]

$$\langle \Phi \rangle = \begin{pmatrix} v_1 & 0 \\ 0 & v_2 e^{i\alpha} \end{pmatrix}, \tag{3}$$

$$\langle \Delta_R \rangle = \begin{pmatrix} 0 & 0 \\ v_R & 0 \end{pmatrix}, \quad \langle \Delta_L \rangle = \begin{pmatrix} 0 & 0 \\ v_L e^{i\theta_L} & 0 \end{pmatrix}, \tag{4}$$

where α and θ_L are called the “spontaneous” CP phase and $v_L \ll v_1^2 + v_2^2 \ll v_R^2$. All the physical effects due to θ_L can be neglected, since this phase is always accompanied by the small v_L .

Under the discrete left-right symmetry the fields transform as follows:

$$\mathcal{P} : \begin{cases} \mathcal{P} f_L \mathcal{P}^{-1} = \gamma_0 f_R \\ \mathcal{P} \Phi \mathcal{P}^{-1} = \Phi^\dagger \\ \mathcal{P} \Delta_{(L,R)} \mathcal{P}^{-1} = -\Delta_{(R,L)} \end{cases} \quad \mathcal{C} : \begin{cases} \mathcal{C} f_L \mathcal{C}^{-1} = C(\bar{f}_R)^T \\ \mathcal{C} \Phi \mathcal{C}^{-1} = \Phi^T \\ \mathcal{C} \Delta_{(L,R)} \mathcal{C}^{-1} = -\Delta_{(R,L)}^* \end{cases} \quad (5)$$

where γ_μ ($\mu = 0, 1, 2, 3$.) are the gamma matrices and \mathcal{C} is the charge conjugation operator.

Lepton masses: lepton masses are due to the following Yukawa interactions (once the Higgs fields take their v.e.v along their neutral components)

$$\mathcal{L}_Y = \bar{L}_L (Y_\Phi \Phi + \tilde{Y}_\Phi \tilde{\Phi}) L_R + \frac{1}{2} (L_L^T C i \sigma_2 Y_{\Delta_L} \Delta_L L_L + L_R^T C i \sigma_2 Y_{\Delta_R} \Delta_R L_R) + h.c., \quad (6)$$

where $\tilde{\Phi} = \sigma_2 \Phi^* \sigma_2$, σ_2 is the Pauli matrix and $C \equiv i \gamma_2 \gamma_0$.

Invariance of the Lagrangian under the Left-Right symmetry requires the Yukawa couplings to satisfy

$$\mathcal{P} : \begin{cases} Y_{\Delta_{R,L}} = Y_{\Delta_{L,R}} \\ Y_\Phi = Y_\Phi^\dagger \\ \tilde{Y}_\Phi = \tilde{Y}_\Phi^\dagger \end{cases}, \quad \mathcal{C} : \begin{cases} Y_{\Delta_{R,L}} = Y_{\Delta_{L,R}}^* \\ Y_\Phi = Y_\Phi^T \\ \tilde{Y}_\Phi = \tilde{Y}_\Phi^T \end{cases} \quad (7)$$

Consistent with the above notation, the neutrino mass matrix of neutrinos is of the form [5,6]

$$\mathcal{L}_\nu = \frac{1}{2} \begin{pmatrix} \nu & N^c \end{pmatrix}_L^T C \begin{pmatrix} M_L & M_D^* \\ M_D^\dagger & M_R \end{pmatrix} \begin{pmatrix} \nu \\ N^c \end{pmatrix}_L + h.c., \quad (8)$$

where $N_L^c \equiv C \bar{N}_R^T$ and M_L , M_R and M_D are 3×3 matrices given by

$$M_L \equiv Y_{\Delta_L} v_L e^{i\theta_L}, \quad (9)$$

$$M_R \equiv Y_{\Delta_R}^* v_R, \quad (10)$$

$$M_D \equiv v_1 Y_\Phi + \tilde{Y}_\Phi v_2 e^{-i\alpha}. \quad (11)$$

After diagonalization, the light and heavy neutrino mass matrices takes the see-saw form:

$$M_\nu \simeq M_L - M_D^* \frac{1}{M_N} M_D^\dagger, \quad (12)$$

$$M_N \simeq M_R. \quad (13)$$

The contributions to the light neutrino masses proportional to M_D and M_L are called the Type I and Type II see-saw contributions respectively. It follows from the seesaw formula that the eigenstates corresponding to Eqs. (12) are given by

$$\begin{pmatrix} \nu' \\ N'^c \end{pmatrix} = \begin{pmatrix} 1 & \Theta \\ -\Theta^T & 1 \end{pmatrix} \begin{pmatrix} \nu \\ N^c \end{pmatrix}, \quad (14)$$

where the heavy-light neutrino mixing is given by

$$\Theta \simeq M_D^* M_N^{-1}. \quad (15)$$

Finally, the charged lepton mass matrix is given by

$$M_l = Y_\Phi v_2 e^{i\alpha} + \tilde{Y}_\Phi v_1. \quad (16)$$

As usual, the mass matrices can be diagonalized by the bi-unitary transformations

$$M_l = U_{lL} \hat{M}_l U_{lR}^\dagger, \\ M_\nu = U_\nu^* \hat{M}_\nu U_\nu^\dagger, \quad M_N = U_N^* \hat{M}_N U_N^\dagger, \quad (17)$$

where \hat{M}_l , \hat{M}_ν and \hat{M}_N are diagonal matrices with real, positive eigenvalues.

Charged gauge interactions with leptons: from the covariant derivative and in the mass eigenstates basis, the charged current Lagrangian is

$$\mathcal{L}_{cc} = \frac{g}{\sqrt{2}} (\bar{l}_L V_L \not{W}_L \nu_L - \bar{l}_L \Theta_L \not{W}_L N_L^c + \bar{l}_R V_R \not{W}_R N_R + \bar{l}_R \Theta_R \not{W}_R \nu_R^c) + h.c., \quad (18)$$

where $N_R \equiv C(\bar{N}_L^c)^T = i\gamma_2\gamma_0(N_L^c)^*$, $\nu_R^c \equiv C(\bar{\nu}_L)^T$ and γ_0 and γ_2 are the gamma matrices and the mixing matrices V_L , V_R , Θ_L and Θ_R are given by

$$V_L = U_{lL}^\dagger U_\nu, \quad \Theta_L = U_{lL}^\dagger \Theta U_N \quad (19)$$

$$V_R = U_{lR}^\dagger U_N^*, \quad \Theta_R = U_{lR}^\dagger \Theta^\dagger U_\nu^* \quad (20)$$

We may use the freedom of rephasing the charged lepton fields to remove three unphysical phases from V_L , which ends up having 3 mixing angles and 3 phases, namely one Dirac and two Majorana phases. Since the freedom of rephasing the charged lepton is already used for V_L , its right-handed analog –the leptonic mixing matrix V_R – is a general 3×3 unitary matrix and may be therefore parametrized by 3 mixing angles and 6 phases.

A comment regarding the mixing matrices Θ_L and Θ_R is in order: for charge conjugation as the LR symmetry, without loss of generality one can choose $U_{lL} = U_{lR} = 1$, such that $V_L = U_\nu$ and $V_R = U_N^*$. In this case, the mixing matrices can be written in the form

$$\Theta_L = \Theta V_R^*, \quad \Theta_R = \Theta V_L^*. \quad (21)$$

For Parity as the LR symmetry, it is no longer true that one can assume $U_{lL} = U_{lR} = 1$. Nevertheless, since the Dirac mass matrix is hermitian with a very good approximation, even in this case one can write

$$\Theta_L = \Theta V_R^* \left[1 + \mathcal{O} \left(\hat{M}_l \tan 2\beta \sin \alpha \right) \right], \quad \Theta_R = \Theta V_L^* \left[1 + \mathcal{O} \left(\hat{M}_l \tan 2\beta \sin \alpha \right) \right]. \quad (22)$$

where the parameter $\tan 2\beta \sin \alpha \lesssim 2m_b/m_t$ [35,36], $\beta \equiv v_2/v_1$, m_b and m_t are the bottom and top quark masses respectively. Therefore, up to small terms of the order $\mathcal{O}(\hat{M}_l \tan 2\beta \sin \alpha)$, the heavy light mixing matrices are roughly the same for both parity and charge conjugation as the LR symmetry.

Heavy-light mixing in the mLRSM: in the mLRSM, the heavy-light neutrino mixing depends on the light and the heavy neutrino mass matrices. It is known [15] that this mixing enters in the decay of the heavy neutrino into a left-handed charged lepton and two jets [14], and one could measure the mixing by measuring the chirality [20] of the outgoing charged lepton in order to discriminate this channel from the usual channel where the heavy neutrino decays into a right-handed charged leptons and two jets¹. Instead, in this work we point out that the same mixing enters in the purely leptonic decay of the heavy neutrinos. This channel has an advantage with respect to the channel with two leptons and two jets, since no asymmetry (chirality information) needs to be measured in order to obtain the heavy-light mixing matrix elements. In addition, from the experimental perspective, the backgrounds relevant to the purely leptonic channel are cleaner. This channel has been previously studied in Refs. [21, 37] including both prompt and displaced vertex for the signal in the context of the SM extended by a fermion singlet. In the latter instance, no heavy resonance W_R is produced in the process, which makes kinematics for the final states very different with respect to the present work.

In what follows and for the sake of illustration, we consider \mathcal{C} as the LR symmetry but the same conclusions hold for the case when the LR symmetry corresponds to \mathcal{P} . From Eq. (7) it follows that the Dirac mass term is symmetric and Eq. (12) takes the form [15]

$$M_\nu \simeq Y_{\Delta_L} v_L e^{i\theta_L} - M_D^* \frac{1}{M_N} M_D^*. \quad (23)$$

Multiplying from the left by M_N^{-1} one gets [38]

$$M_N^{-1} M_\nu \simeq M_N^{-1} Y_{\Delta_L} v_L e^{i\theta_L} - \frac{1}{M_N} M_D^* \frac{1}{M_N} M_D^*, \quad (24)$$

$$M_N^{-1} M_\nu \simeq M_N^{-1} M_L - \Theta^2. \quad (25)$$

Hence, the mixing angle can be written in terms of the heavy and light neutrino masses as [38]

$$\Theta = \sqrt{\epsilon - M_N^{-1} M_\nu} = M_D^* M_N^{-1}, \quad (26)$$

with $\epsilon \equiv v_L/v_R$. See Ref. [16, 17] for the determination of the analogue of Eq. (26) for Parity as the LR symmetry. In what follows and for the sake of simplifying the discussion, we set $v_L = 0$,

¹The relative strength of these two channels can be seen for instance from the "phase diagram" of the heavy-light mixing in the see-saw models in Ref. [31], and it is pointed out that without special Yukawa texture the ordinary channel with heavy neutrino decay with right-handed charged current is generally much larger than the left-handed current.

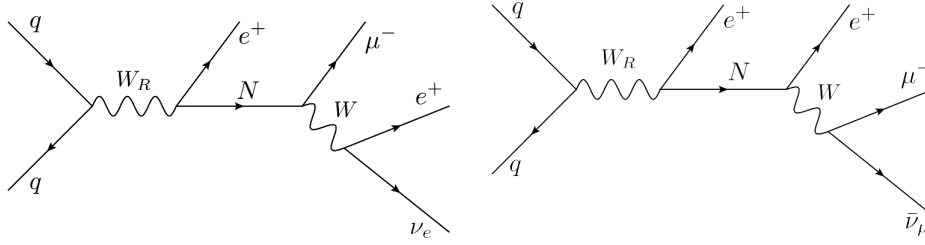


Figure 1: Feynman diagrams for the W_R production and leptonic decay $N \rightarrow e^+ \mu^- \nu$, where ν can be either a ν_e or $\bar{\nu}_\mu$.

effectively assuming type I see-saw dominance for the light neutrino masses. Notice that the choice v_L small is technically natural, as discussed originally in Ref. [6] and more recently revisited in Ref. [39]. Finally, notice that the mixing matrix Θ (equivalently M_D) is a complex matrix, so that no issues arise due to the -1 factor inside the square root and the fact that ϵ is a complex quantity. In any case, this phase factor has no impact in our analysis below. For a discussion of its physical significance see, for instance, Ref. [38].

In the next section and using the above leptonic channel, we study the sensitivity of the LHC, HE-LHC and a 100 TeV pp collider, to the mixing in Eq. (26) as a function of M_{W_R} and the lightest heavy neutrino mass m_N , for benchmark values of the other heavy neutrinos. Later, from this sensitivity and using Eq. (15), one can infer the values of M_D that can be probed at the LHC and the next generation of hadronic colliders.

2.2 “Non minimal” left-right symmetric model

As explained in the previous section, in the mLRSM the gauge group is broken to the SM group through the triplet Δ_R and the bidoublet scalar Φ . This construction generates a seesaw mass for the right-handed neutrinos from the vacuum expectation value of the Δ_R . Here, we will consider a slightly different LR scenario, a “non-minimal” model, in which now the LR group is broken through a doublet scalar in the $(1,2,-1)$ representation of \mathcal{G} [40,41]. Adding an extra vector of gauge singlet fermions $S = (S_1, S_2, S_3)^T$ to the particle content the neutrino masses will be generated now by an inverse seesaw mechanism [42,43]. The inverse seesaw scenario in the context of left-right symmetry was studied in detail in Ref. [44]. In this section, we will only review the most important results.

We work in the basis in which the charged lepton mass matrix is diagonal. The inverse seesaw neutrino mass matrix in the interaction basis for the neutral states $\mathcal{N} = (\nu_L, N^c, S^c)^T$ can be written in a 3×3 notation as:

$$\mathcal{M} = \begin{pmatrix} 0 & M_D^T & 0 \\ M_D & 0 & M_N \\ 0 & M_N^T & \mu \end{pmatrix} \quad (27)$$

where M_D , M_N , and μ denote 3×3 matrices and the sub-matrix μ is taken to be diagonal. Assuming the sub-matrices M_D , M_N , μ have mass scales arranged hierarchically, $M_N \gg M_D$, μ , the light neutrino mass matrix M_ν can be expressed in terms of the matrices in Eq. (27) as

$$M_\nu \simeq M_D^T \frac{1}{M_N^T} \mu \frac{1}{M_N} M_D. \quad (28)$$

Using the bi-unitary transformations

$$M_\nu = V_L^* m_\nu V_L^\dagger, \quad M_N = V_R \hat{M}_N U_R^\dagger, \quad (29)$$

the mass matrix \mathcal{M} can be diagonalized into

$$\hat{\mathcal{M}} = \begin{pmatrix} m_\nu & 0 & 0 \\ 0 & \hat{M}_N^- & 0 \\ 0 & 0 & \hat{M}_N^+ \end{pmatrix}. \quad (30)$$

Here \hat{M}_N^- , \hat{M}_N^+ and \hat{M}_N are diagonal mass matrices with $\hat{M}_N^\pm = \hat{M}_N \pm \frac{1}{2}\mu^V$ and $\mu^V = V_R^T \mu V_R$. The neutral mass eigenstates $\mathcal{N}' = (\nu, N_-, N_+)^T$ correspond to three light neutrinos and three pairs of almost degenerate heavy neutrinos with mass eigenvalues $m_{N_i^\pm} = (\hat{M}_N^\pm)_{ii} = (\hat{M}_N)_{ii} \pm \frac{1}{2}(\mu^V)_{ii}$.²

Using Eqs (28), (29) the light neutrino mass matrix can be written as

$$m_\nu = V_L^T M_D^T \frac{1}{M_N^T} \mu \frac{1}{M_N} M_D V_L. \quad (31)$$

Following the parameterization developed by Casas and Ibarra [18] we can now write M_D as:

$$M_D = M_N \frac{1}{\sqrt{\hat{\mu}}} \mathcal{R} \sqrt{m_\nu} V_L^\dagger. \quad (32)$$

Here the matrix \mathcal{R} is an arbitrary complex orthogonal matrix. Rewriting M_N using Eq. (28) one finds:

$$V_R^\dagger M_D = \hat{M}_N U_R^\dagger \frac{1}{\sqrt{\hat{\mu}}} \mathcal{R} \sqrt{m_\nu} V_L^\dagger, \quad (33)$$

which express $V_R^\dagger M_D$ in terms of the low energy observables m_ν , V_L allowing us to reproduce the neutrino data. Notice that in practice, the arbitrariness of the matrix \mathcal{R} is a consequence of the fact that for the non-minimal models, the Dirac mass matrix is arbitrary. This feature precludes a direct mapping of neutrino data onto M_D in non-minimal models.

²Here the three pairs of – almost degenerate – neutrinos correspond to the so-called ”quasi-Dirac” neutrinos [23, 44, 45].

The mixing matrix \mathcal{V} that relates the neutral mass eigenstates \mathcal{N}' and the interaction eigenstates \mathcal{N} via $\mathcal{N} = \mathcal{V} \mathcal{N}'$ can be expressed in the seesaw approximation as [44]:

$$\mathcal{V} \simeq \begin{pmatrix} V_L & i\Theta_L & \Theta_L \\ 0 & -\frac{i}{2}V_R^* & \frac{1}{2}V_R^* \\ -\sqrt{2}U_R\Theta_L^\dagger V_L & \frac{i}{\sqrt{2}}U_R & \frac{1}{\sqrt{2}}U_R \end{pmatrix}, \quad (34)$$

where $\Theta_L = \frac{1}{\sqrt{2}}M_D^\dagger V_R \hat{M}_N^{-1}$.³

3 Collider sensitivities

As discussed in the previous section, the most promising channel for the determination of the Dirac Yukawa coupling of neutrinos is the purely leptonic channel $pp \rightarrow W_R^\pm \rightarrow l^\pm l^\pm l^\mp \nu$. For purposes of illustration, we focus on the process $pp \rightarrow e^+ N \rightarrow e^+ \mu^- e^+ \nu$ (see Fig. 1) rather than $pp \rightarrow \mu^+ N \rightarrow \mu^+ e^- e^+ \nu$ in order to avoid the presence of an $e^+ e^-$ pair in the final state. The final state with different flavors for leptons of the same charge has a cleaner Standard Model background and also avoids events coming from the heavy neutrino decaying through the neutral currents (for example $pp \rightarrow W_R^+ \rightarrow e^+ N \rightarrow e^+ \nu Z_{(R)}^* \rightarrow e^+ e^+ e^- \nu$).

We study the main sources of background for the process $pp \rightarrow e^+ N \rightarrow e^+ \mu^- e^+ \nu$ for different center of mass energies. In what follows, we discuss the LHC expected sensitivity to the branching ratio of HNs decaying into leptons at the LHC with $\sqrt{s} = 13$ TeV, the high energy LHC (HE-LHC) with $\sqrt{s} = 28$ TeV and a pp collider with $\sqrt{s} = 100$ TeV. We compare our cross section results with those obtained in Refs. [15, 16, 46, 47] for the $pp \rightarrow e^+ N$ production and find agreement.

Assuming that the neutrinos in the final state cannot be distinguished, the decay width of heavy neutrinos into three leptons $\Gamma(N \rightarrow l^\pm l'^\mp \nu)$ is proportional to the heavy-light mixing and it is of the form

$$\Gamma(N \rightarrow l^\pm l'^\mp \nu) = (|(\Theta_L)_{lN}|^2 + |(\Theta_L)_{l'N}|^2) \frac{G_F^2}{96\pi^4 m_N} \int_0^{m_N^2} dx \frac{\pi(m_N^2 - x)(m_N^4 + x m_N^2 - 2x^2)}{m_N^2 (1 - \frac{x}{M_W^2})^2}. \quad (35)$$

Where m_N denotes the mass of the heavy neutrino.⁴ For illustration we assume $V_L = V_R^*$ and the indicative upper limit on light neutrino masses $\sum_\nu m_\nu = 0.5$ eV [48]. In Figure 2 we show the branching ratio of the heavy neutrino N into $e^+ \mu^- \nu$ as a function of the lightest heavy neutrino (HN) mass in the minimal left-right symmetric model. As can be seen from the figure, the branching ratio into leptons decreases as the heavy neutrino mass m_N increases.

³The expressions of the couplings of the heavy neutrinos to the gauge bosons are given in [44].

⁴In the inverse seesaw scenario, m_N denotes collectively the pair of mass eigenvalues $m_{N\pm}$ for $N = N_\pm$.

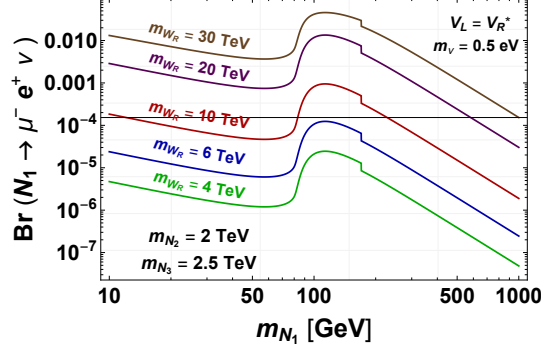


Figure 2: Branching ratio of the purely leptonic decays of the heavy neutrino N in the minimal left-right symmetric model. We use the indicative limit for light neutrino masses of $m_\nu = 0.5$ eV [48].

This feature is due to the proportionality of the leptonic branching ratio to Θ_L^2 (see Eq. (35)), which in turn is proportional to $1/m_N$ —see Eq. (26).

Another important feature is the increase of the leptonic branching ratio as the W_R boson mass increases. This occurs because the dominant process with one lepton and two jets has an additional suppression of M_{W_R} . The net effect is to make the branching ratio into leptons increase when the W_R boson mass increases. Finally, the bump when $m_N \sim M_W$ is due to the transition from three body decay to a two-body decay through an on-shell W boson. The drop in the decay rate due to the top quark threshold is also evident.

Regarding the processes shown in Fig. 1, we find two issues that may affect the selection efficiency of the signal: (1) the two origins of the μ^- , which is an interpretation issue and (2) the possible jet fake background:

1. The origin of the μ^- : there are two possibilities

$$pp \rightarrow e^+ N \rightarrow e^+ \mu^- (W^+ \rightarrow e^+ \nu_e), \quad (36)$$

and

$$pp \rightarrow e^+ N \rightarrow e^+ e^+ (W^- \rightarrow \mu^- \bar{\nu}_\mu). \quad (37)$$

Namely, the final state muon can be directly produced in the decay of the heavy neutrino N or it can also be produced in the decay of the W boson that comes from the decay of the heavy neutrino N . Notice that the lepton flavor cannot be used to discriminate among the two processes since the light neutrino goes undetected.

For $m_N > m_W$, the transverse mass of the subleading positron and missing transverse energy \cancel{E}_T system $m_T(e_{sub}^+ \cancel{E}_T)$ may be helpful for discriminating between the two processes. In the process in Eq. (36) the subleading positron comes primarily from the decay

of an on-shell W boson, so the transverse mass of the subleading positron and missing transverse energy system will have a sharp decline around the mass of the W boson. On the contrary, in the process in Eq. (37), the subleading positron directly comes from the decay of heavy neutrino N , so one may expect a broader distribution of this transverse mass. In principle, then, implementing a cut on this transverse mass near m_W should remove a significant portion of events from the process in Eq. (37) while retaining most events coming from the process in Eq. (36). We expect this method will be useful for $m_N \gg m_W$, but will be of less utility for m_N near m_W . In the latter regime, the transverse mass mentioned above will be narrow in both processes, and, therefore, not efficient in discriminating between these two processes. We will return to this point below and show the distribution of this transverse mass for different benchmarks in Fig. 3.

For $m_N < m_W$ the decay goes through an off-shell W boson. In this case, it seems at first glance more difficult to distinguish between these two contributions. In principle, one cannot determine the origin of the muon for a single event. However, a way to determine the proportion of μ^- from each channel by measuring a particular forward-backward asymmetry with an ensemble of events has been proposed in Ref. [49]. In this work, we follow a different approach. In both cases mentioned above, when deriving the sensitivity to the decay branching ratio $\text{Br}(N \rightarrow e^+e^+\mu^-\nu)$, we first estimate the efficiency for each channel shown in Fig. 1 (see Fig. 4) and subsequently compute the average efficiency by weighting each channel with the corresponding probability of occurrence.

2. Since the mixing parameter Θ_L may be quite small, there may be a non-negligible jet-fake background coming from the process $pp \rightarrow W_R^\pm \rightarrow l^\pm l^\pm jj$, where one of the jets is misidentified as either an electron or a muon, since we did not reject extra jets in our analysis. Notice that the branching ratio for this channel is by far the dominant one. Therefore, it can mimic the purely leptonic signal with one of the jets faking to leptons, which may be a contamination and decrease the sensitivity to the heavy-light mixing. As discussed below, we address this issue by implementing cuts on the missing transverse energy E_T and the transverse mass of the subleading electron and E_T system. We find that for heavy neutrino masses $m_N < 1$ TeV, this channel is subdominant with respect to the trilepton channel.

For the signal generation, we use the extension of the FeynRules package [50] for the minimal LR model used in Ref. [51] and expanded in Ref. [52]. The signal and background events were generated at LO using Madgraph 5 [53], Pythia 6 [54] for hadronization, and Delphes 3 [55] for detector simulation, using the JetFake module developed in [52]. The dominant sources of background are found to be $t\bar{t}W$, $t\bar{t}(j)$ (with a jet faking a lepton) and $WWW(j)$, while $WZ(j)$, $t\bar{t}Z$ and $Z/\gamma(j)$ (with charge flip and a jet faking a muon) are sub-dominant. The

Cut description	
$e^+e^+\mu^-$, no b jets and no additional leptons	signal selection
$p_{T,e^+}^{lead} > 200$ GeV, $p_{T,e^+}^{sub} > 100$ GeV, $p_{T,\mu^-}^{lead} > 100$ GeV	reduce all backgrounds
$\cancel{E}_T > 100$ GeV	reduce mostly $t\bar{t}(j)$ and $Z/\gamma(j)$
$ m_{inv}(e^+e^+) - 91.2 > 10$ GeV	reduce mostly $WZ(j)$
$m_T(e_{sub}^+ \cancel{E}_T) < 150$ GeV	select channel shown in Fig. 1 (right)
$m_T(e^+e^+\mu^- \cancel{E}_T) > M_{W_R}/2$	reduce all backgrounds

Table 1: Selection criteria used to reduced the SM background for 100 TeV. For 13 TeV and 28 TeV we apply the same cuts, excepting that $p_{T,e^+}^{lead} > 100$ GeV.

j in the parenthesis means that we generated the corresponding background with one matched jet. Tables 2, 3 and 4 show the cut flow (see below) for the main sources of background for this process, together with two signal benchmark points, for 13 TeV, 28 TeV and 100 TeV respectively. As already remarked, we assume the left and right leptonic mixing matrix to satisfy $V_L = V_R^*$. Some of the backgrounds for this process were studied in Ref. [22]. In our analysis, further sources of backgrounds are included mostly due to the charge misidentification probability that becomes more important at higher p_T . We compare our WZ and triple boson (WWW) backgrounds with the CMS estimates from Ref. [22]. In particular, we compare with the second last bin in the left panel of Figure A.3 from Ref. [22], which turns out to be closer to the kinematic region in our analysis, and find an agreement for WZ and about half of the yield for the WWW background. This difference is consistent with the 50% uncertainty quoted for the estimate for triboson production.

A description of the selection criteria is shown in Table 1. We first demand that each event contains exactly two positrons, one muon, and no b -tagged jets. Events with extra jets that are not b -tagged are retained. Secondly, we select events with high transverse momentum p_T for the leptons and large missing transverse energy \cancel{E}_T in order to reduce many of the backgrounds. Then we require the reconstructed invariant mass of the positron pair $m_{inv}(e^+e^+)$ to be outside the Z boson mass peak, reducing the background coming from $Z \rightarrow e^+e^-$ when the electron charge is misidentified.

The next cut in Table 1 is on the transverse mass of the positron and missing energy $m_T(e_{sub}^+ \cancel{E}_T)$. We enforce the reconstructed transverse mass of the sub-leading positron and missing energy to be less than 150 GeV. In principle, if the momentum of the leptons are exactly reconstructed, then $m_T(e_{sub}^+ \cancel{E}_T)$ will not exceed the mass of the W boson. However, due to smearing effects, the distribution of this transverse mass is broadened. This is why we choose the cut on this variable to be larger than the W boson mass. In Fig. 3 we show the $m_T(e_{sub}^+ \cancel{E}_T)$ distribution for different masses of the heavy neutrino N_1 and $M_{W_R} = 6$ TeV for a 100 TeV pp-collider. One can observe from these distributions that imposing a cut on this transverse

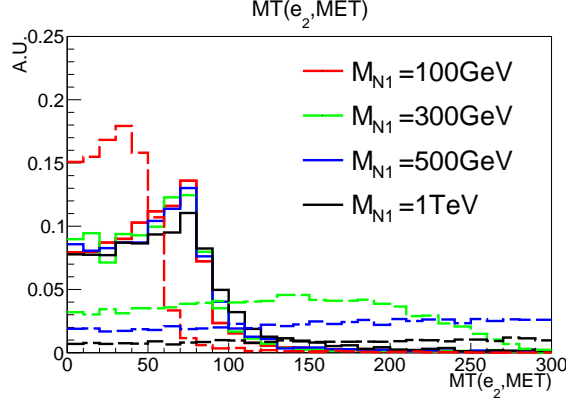


Figure 3: The distribution of the transverse mass of the subleading positron and missing E_T at 100 TeV pp-collider with benchmark point $M_{W_R} = 6$ TeV, $m_{N_2} = 2$ TeV, $m_{N_3} = 2.5$ TeV. Different colors represents different masses of m_{N_1} , the solid and dashed curves represent the events coming from the left and right diagram in Fig. 1 respectively.

mass can effectively discriminate the two diagrams in Fig. 1 if the mass of the N_1 is sufficiently large. As noted earlier, this discrimination can be achieved because the positron from the heavy neutrino decay comes mostly from an on-shell W boson decay in the process in Eq. (37). The signal efficiencies are different for the two processes in Fig. 1. In Fig. 4 we show the signal efficiency for each channel individually as well as the averaged efficiencies with different relative strength of the two channels characterized by the parameter r defined below:

$$r \equiv \frac{Br(N_1 \rightarrow e^+(W^- \rightarrow \mu^- \bar{\nu}_\mu))}{Br(N_1 \rightarrow \mu^-(W^+ \rightarrow e^+ \nu_e))}. \quad (38)$$

As one can see from the left plot in Fig. 4, the efficiency of the channel shown in Eq. (37) decreases as the mass of the N_1 increases. This is mainly due to the cut $m_T(e_{sub}^+ \cancel{E}_T) < 150$ GeV shown in Table 1, which helps to discriminate between the two channels shown in Eqs. (36) and (37).

The last selection in Tab. 1 is a cut on the transverse mass of the $e^+e^+\mu^- \cancel{E}_T$ system, since for an on-shell W_R boson, the transverse mass distribution is peaked at M_{W_R} (see Fig. 5), where the SM backgrounds give a negligible contribution. The rejection of the backgrounds was effectively achieved by using the cut $m_T(e^+e^+\mu^- \cancel{E}_T) > M_{W_R}/2$ shown in Table 1. In this way, most of the signal events are kept while a significant portion of the backgrounds is rejected. Furthermore, this cut also guarantees that the SM backgrounds become even more suppressed when searching for a W_R boson with higher mass.

For the charge flip probability, we take the current ATLAS performance in Ref. [56], which parameterizes the flip probability P as the product of functions of η and P_T : $P = f(\eta) \times \sigma(P_T)$. Also we assume that $\sigma(P_T)$ for $P_T > 400$ GeV keeps the same value as that in the bin (200,400)

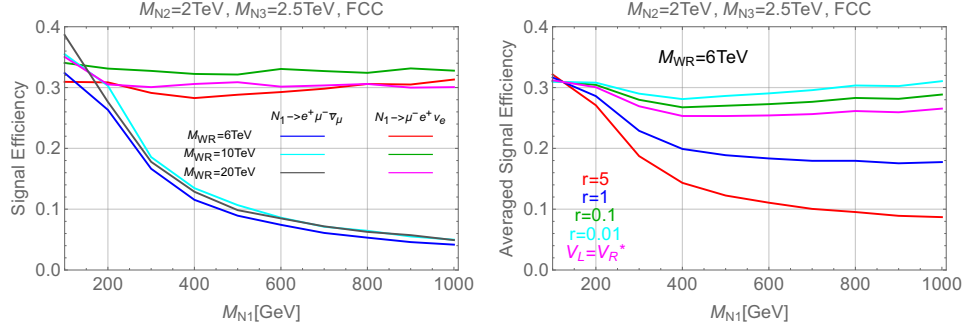


Figure 4: The signal efficiencies for the benchmark point: $m_{N_2} = 2 \text{ TeV}$, $m_{N_3} = 2.5 \text{ TeV}$. The left plot shows the signal efficiencies for each channel with different mass of W_R and N_1 . The right plot shows the signal efficiencies for different relative strengths r of the two channels (defined in Eq. 38), with $M_{W_R} = 6 \text{ TeV}$.

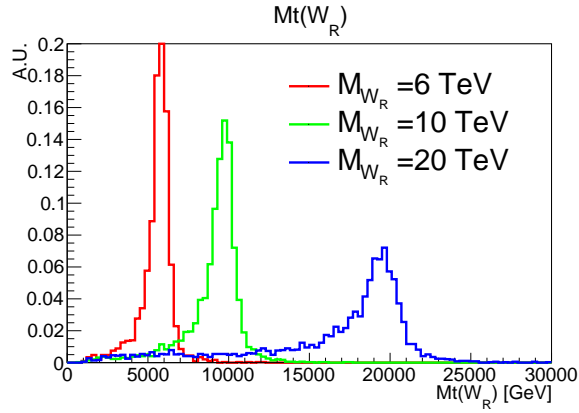


Figure 5: The distribution of the reconstructed transverse mass of W_R at a 100 TeV pp-collider, with benchmark point $m_{W_N} = 300 \text{ GeV}$, $m_{N_2} = 2 \text{ TeV}$, $m_{N_3} = 2.5 \text{ TeV}$. Different colors represents different masses of W_R .

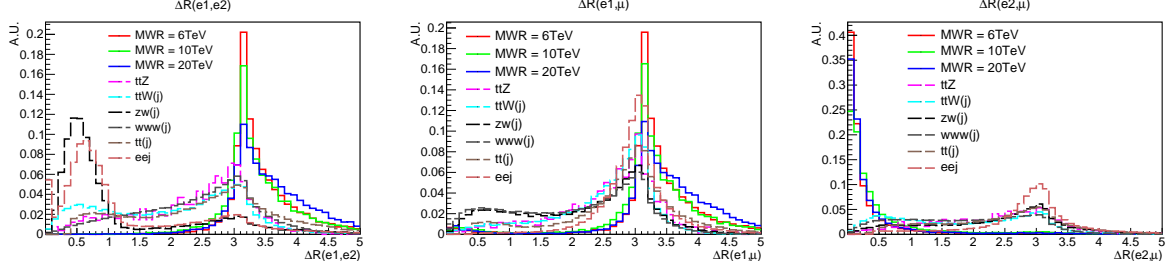


Figure 6: ΔR for the decay products of the process shown in Fig. 1. e_1 and e_2 refers to the harder and softer positrons sorted by transverse momentum. We assume $m_N = 100$ GeV and plot the signal for different values of M_{W_R} .

GeV. For our analysis of the 100 TeV collider reach, we use the same charge flip probability, as we are not aware of a more realistic estimation having appeared in the literature to date.

Finally, a comment on a possible future refinement that can be made in the analysis and that exploits a particular kinematic feature of the signal. For HN masses much smaller than the W_R boson mass, the decay products coming from the HN are merged and form what it has been coined as a *lepton jet* [21]. In Fig. 6, we show $\Delta R \equiv \sqrt{\Delta\phi^2 + \Delta\eta^2}$ for the decay products of the process shown in Fig. 1. Since $\Delta R(\mu e_2)$ for the signal is peaked at smaller values (around $\Delta R \sim 5 \times 10^{-2}$ for $m_N = 100$ GeV and for $M_{W_R} = 6, 10, 20$ TeV) than $\Delta R(\mu e_1)$ and $\Delta R(e_1 e_2)$, we see that the positron with smaller energy is mainly coming from the HN decay. This kinematic variable has been previously proposed in Ref. [31]. Although we did not need to use this kinematic feature in our analysis, it is worth to keep it in mind, since it is one of the more distinctive topological features of the signal in the mass range considered in this work and it may be used to reject further backgrounds.

3.1 Sensitivity at the LHC

The LHC sensitivity to the branching ratio into the purely leptonic channel is shown in Fig. 7, with the corresponding cut flow for representative two signal points given in Table 2⁵. In our calculations we assumed $V_L = V_R^*$ and set $\mathcal{R} = U_R = I$, $\mu = 10^{-4}$ GeV for the non-minimal model. This choice of parameters corresponds to $r \sim 1$ in both scenarios.⁶ As expected the maximum reach is obtained for $M_{W_R} = 4$ TeV, for a wide range of the heavy neutrino mass, with the branching ratio reach extending down to $\sim 10^{-2}$ at 2σ significance. The solid blue

⁵In this analysis, we studied the sensitivity of the trilepton signal for masses $m_N \gtrsim 80$ GeV. A similar analysis can be carried out for smaller masses, although in this case the N could decay with a displaced vertex, as previously studied in Refs. [47, 57–60]

⁶In the inverse see saw scenario different values of $r \sim [0, 1]$ are possible even if we assume $V_L = V_R^*$. This is because the lepton number violating process $pp \rightarrow W_R^+ \rightarrow e^+ e^+ \mu^- \bar{\nu}_\mu$ in Eq. (37) might be suppressed with respect to the lepton number conserving process $pp \rightarrow W_R^+ \rightarrow e^+ \mu^- e^+ \nu_e$ in Eq. (36) for $\mu < \Gamma_N$, being Γ_N the decay width of the heavy neutrino (see the discussion in Refs. [44, 61]).

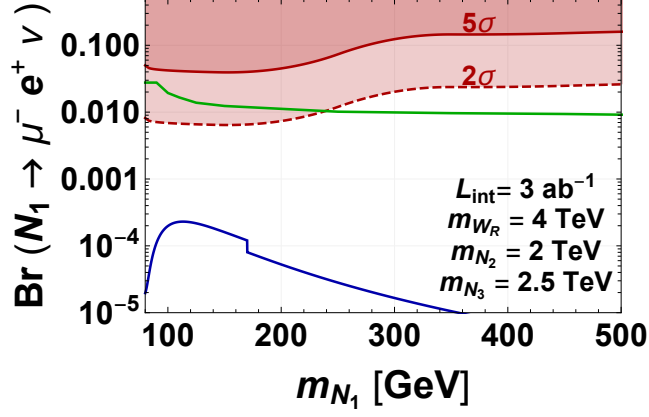


Figure 7: LHC reach to the branching ratio of the purely leptonic decays of the heavy neutrino. The blue (green) line denotes the branching ratio within the minimal (non-minimal) LR model and the shadowed thick(dashed) regions show the reach at $5\sigma(2\sigma)$, for an integrated luminosity of $L_{int} = 3\text{ab}^{-1}$ and center of mass energy $\sqrt{s} = 13\text{ TeV}$. We assume $V_L = V_R^*$ and the upper limit on light neutrino masses of $m_\nu = 0.5\text{ eV}$ [48]. For the non-minimal model we have set $\mathcal{R} = U_R = I$ and $\mu = 10^{-4}\text{ GeV}$.

$\sqrt{s}=13\text{TeV}$	Backgrounds						Signal	
	$t\bar{t}Z$	$t\bar{t}W$	$t\bar{t}(j)$	$WZ(j)$	$3W$	$Z/\gamma(j)$	$m_N(100\text{ GeV})$	$m_N(500\text{ GeV})$
$e^+e^+\mu^-$ (b-veto)	11.8	74.9	23058	24.8	6.71	901	1293	371
P_T cuts	0.325	3.75	216	0.215	2.33	5.31	825	253
\cancel{E}_T GeV	0.158	1.85	117	0.0761	1.06	0.0911	646	188
$m_{inv}(e^+e^+)$	0.155	1.82	113	0.0761	1.05	0	646	188
$m_T(e_{sub}^+ \cancel{E}_T)$	0.0582	0.743	48.4	0.0277	0.491	0	622	176
$m_T(e^+e^+\mu^- \cancel{E}_T)$	0	7.82×10^{-3}	0	0	0.0169	0	597	158

Table 2: SM background processes at 13 TeV and 3ab^{-1} for the trilepton signal $e^+e^+\mu^-\nu$ and $M_{W_R} = 4\text{ TeV}$, for two benchmark values of the heavy neutrino masses assuming $(\Theta_L)_{\mu N} = (\Theta)_{eN} = \frac{1}{\sqrt{2}}$. Backgrounds ending with (j) were simulated with one matched jet. The charge misidentification probability has been taken from current ATLAS result from Ref. [56].

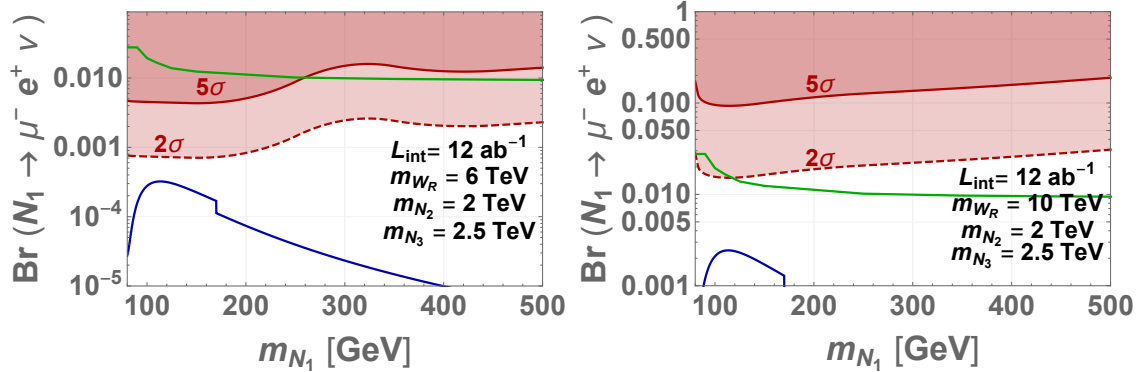


Figure 8: HE-LHC reach to the branching ratio of the purely leptonic decays of the heavy neutrino. The blue (green) line denotes the branching ratio within the minimal (non-minimal) LR model and the shadowed thick(dashed) regions show the reach at $5\sigma(2\sigma)$, for an integrated luminosity of $L_{int} = 12\text{ab}^{-1}$ and center of mass energy $\sqrt{s} = 28$ TeV. We assume $V_L = V_R^*$ and the upper limit on light neutrino masses of $m_\nu = 0.5$ eV [48]. For the non-minimal model we have set $\mathcal{R} = U_R = I$ and $\mu = 10^{-4}$ GeV.

and green curves show the expected branching ratios in the mLRSM and non-minimal models, respectively. It is clear that for the mLRSM, the branching ratio lies well below the sensitivity the HL-LHC ($L_{int} = 3\text{ab}^{-1}$). This suppression with respect to the LHC reach follows from the small values of M_D/M_N needed for consistency with the observed small scale of the light neutrino masses that imply, in turn, small values of the heavy-light neutrino mixing angle. This suppression is not necessarily true in an inverse seesaw scenario. In the latter case, the smallness of the neutrino masses can be attributed to small values of the μ parameter (see Eq. (31)) without requiring the exceedingly small values of M_D/M_N [23, 44, 61]. This feature can be seen explicitly in Fig. 7, where we have obtained the green curve by choosing $\mu = 10^{-4}$ GeV. Therefore, we can conclude that a signal of the purely leptonic channel at the LHC would be an indication of a non-minimal realization of the LR symmetry.

3.2 Sensitivity at the HE-LHC

We now consider the reach of the proposed energy upgrade of the LHC to 28 TeV center of mass energy (HE-LHC). In Fig. 8 we show the expected reach at the HE-LHC for two values of the W_R boson mass. We see from the figure that heavy light mixing can be excluded at 2σ for heavy-light mixing of the order of 10^{-3} for $M_{W_R} = 6$ TeV and of the order of 10^{-2} for $M_{W_R} = 10$ TeV. As in the case of the high luminosity LHC (HL-LHC), the minimal LR scenario is not expected to give any observable signal in the purely leptonic channel, so a positive signal would point to a non-minimal realization of the LR model. Finally and for the purpose of illustration, in Table 3 we show the cut flow for the main background processes and two benchmark points

	Backgrounds						Signal	
$\sqrt{s}=28\text{TeV}$	$t\bar{t}Z$	$t\bar{t}W$	$t\bar{t}(j)$	$WZ(j)$	$3W$	$Z/\gamma(j)$	$m_N(100\text{ GeV})$	$m_N(500\text{ GeV})$
$e^+e^+\mu^-$ (b-veto)	286	882	615657	440	56.6	3139	8766	3208
P_T cuts	9.93	60.0	8791	6.3	22.9	37.9	7000	2474
\cancel{E}_T GeV	5.18	34.1	5115	2.29	12.2	2.33	6037	2092
$m_{inv}(e^+e^+)$	5.00	33.6	4986	2.29	12.2	0.608	6037	2092
$m_T(e_{sub}^+\cancel{E}_T)$	2.14	13.7	2297	0.497	5.83	0	5678	1883
$m_T(e^+e^+\mu^-\cancel{E}_T)$	0	0.028	3.00	0	0.13	0	5555	1800

Table 3: SM background processes at 28 TeV and 12 ab^{-1} for the trilepton signal $e^+e^+\mu^-\nu$ and $M_{W_R} = 6\text{ TeV}$, for two benchmark values of the heavy neutrino masses assuming $(\Theta_L)_{\mu N} = (\Theta)_{eN} = \frac{1}{\sqrt{2}}$. Backgrounds ending with (j) were simulated with one matched jet. The charge misidentification probability has been taken from current ATLAS result from Ref. [56].

	Backgrounds						Signal	
$\sqrt{s}=100\text{TeV}$	$t\bar{t}Z$	$t\bar{t}W$	$t\bar{t}(j)$	$WZ(j)$	$3W(j)$	$Z/\gamma(j)$	$m_N(100\text{ GeV})$	$m_N(500\text{ GeV})$
$e^+e^+\mu^-$ (b-veto)	199	1.1K	1.2K	9K	735	1.1K	1.9M	1.8M
P_T cuts	18.7	387	226	2.4K	254	244	1.34M	1.30M
\cancel{E}_T	12.6	312	138	1.1K	165	18.7	1.1M	1M
$m_{inv}(e^+e^+)\text{cuts}$	12.1	311	136	122	164	5.19	1.1M	1M
$m_T(e_{sub}^+\cancel{E}_T)$	4.42	116	65.1	22	85.9	0.344	1.1M	0.99M
$m_{inv}(e^+e^+\mu^-\cancel{E}_T)$	0.126	7.60	5.82	0.336	9.72	0.0275	1M	0.97M

Table 4: SM background processes at 100 TeV and 30 ab^{-1} for the trilepton signal $e^+e^+\mu^-\nu$ and $M_{W_R} = 6\text{ TeV}$, for two benchmark values of the heavy Neutrino masses assuming $(\Theta_L)_{\mu N} = (\Theta)_{eN} = \frac{1}{\sqrt{2}}$. Backgrounds ending with (j) were simulated with one matched jet. The charge misidentification probability has been taken from current ATLAS result from Ref. [56]. The jet to lepton fake rates for $t\bar{t}(j)$ and $Z/\gamma(j)$ have been taken as 10^{-4} universally. The NLO K-factor for backgrounds are taken from Ref. [62]

for the signal.

3.3 Sensitivity at the 100 TeV pp collider

We now turn to the reach of a 100 TeV pp collider, as shown in Fig. 9. The corresponding cut flow is given in Table 4.

In contrast to the situations for the HL-LHC and HE-LHC, a 100 TeV pp collider could observe the trilepton channel for a sufficiently light W_R . As one increases the W_R mass, the range of HN masses for which the trilepton channel is accessible decreases. From the left panel of Fig. 9, we see that for $M_{W_R} = 6\text{ TeV}$ the purely leptonic signal can be discovered(excluded) with $5\sigma(2\sigma)$ sensitivity for heavy neutrino masses below 300 GeV(450 GeV). It is, thus, possible that one might discover the W_R boson at the LHC (with $M_{W_R} < 6\text{ TeV}$) using the two lepton

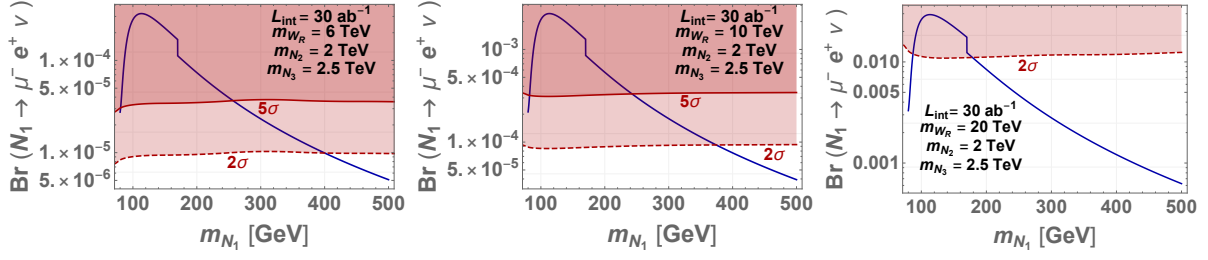


Figure 9: 100 TeV pp collider reach to the branching ratio of the purely leptonic decays of the heavy neutrino. The blue line denotes the branching ratio within the mLRSM and the shadowed thick(dashed) regions show the reach at $5\sigma(2\sigma)$, for an integrated luminosity of $L_{int} = 30\text{ab}^{-1}$ and center of mass energy $\sqrt{s} = 100$ TeV. We assume $V_L = V_R^*$ and the upper limit on light neutrino masses of $m_\nu = 0.5$ eV [48].

and two jets channel [47] yet require a 100 TeV pp collider to probe the HN mass generation by measuring the trilepton signal. For heavier W_R masses, both discovery of the RH W boson and testing the mLRSM Yukawa sector would require a next generation collider. For $M_{W_R} = 10$ TeV, for example, the purely leptonic signal can be discovered(excluded) with $5\sigma(2\sigma)$ sensitivity for heavy neutrino masses below 260 GeV(400 GeV). Finally, for $M_{W_R} = 20$ TeV heavy neutrino masses up to 200 GeV can be excluded at 2σ .

4 Connection between the Dirac mass, the heavy and light neutrino masses and low energy experiments

In this section, we discuss what the expected sensitivity obtained in the previous section implies for the Dirac mass term of the minimal model. Summarizing, we have the two following important points regarding the connection between the Dirac mass and the heavy and light neutrino masses:

1. The trilepton search can determine the mixing between the heavy and light neutrinos Θ_L in Eqs. (21) and (22) which, then, can be related to the Dirac mass M_D using Eq. (15) once M_N is known. The same conclusions apply for the non-minimal setup, where the heavy light mixing is of the form $\Theta_L = \frac{1}{\sqrt{2}} M_D^\dagger V_R \hat{M}_N^{-1}$ – see Eq. (34).
2. The connection between Θ_L , M_D , M_N and M_ν is direct in the minimal model, as can be seen, for instance, from Eq. (26) for \mathcal{C} as the LR symmetry. In the non-minimal model, relating experimentally accessible neutrino mass parameters with the Lagrangian mass parameters is far less direct due to the arbitrary, complex, orthogonal matrix \mathcal{R} shown in Eq. (33).

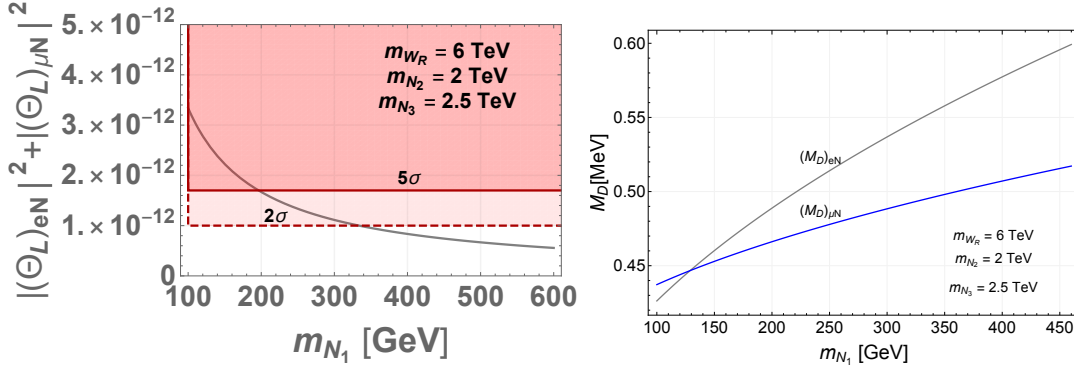


Figure 10: Value for the heavy-light mixing angle combination $|\Theta_{N\mu}|^2 + |\Theta_{Ne}|^2$ (right) and the Dirac Mass M_D (left) as a function of the heavy neutrino mass, for $M_{W_R} = 6$ TeV for a 2σ exclusion region shown in Fig. 9. We assume $V_L = V_R^*$ and the upper limit on light neutrino masses of $m_\nu = 0.5$ eV [48].

Therefore and for the mLRSM, it is interesting to compare the exclusion lines obtained in Fig. 9 with the prediction one can make in this case. In Fig. 10 (left panel) we plot the combination $|(\Theta_L)_{N\mu}|^2 + |(\Theta_L)_{Ne}|^2$ given by Eq. (15), as a function of m_N together with the 2σ and 5σ significance regions expected at the 100 TeV pp collider. We see that at the 100 TeV pp collider, the heavy-light mixing Θ can be probed for values as small as $|(\Theta_L)_{N\mu}|^2 + |(\Theta_L)_{Ne}|^2 \sim 10^{-12}$. Notice that since $|(\Theta_L)_{N\mu}|^2 + |(\Theta_L)_{Ne}|^2 \sim 10^{-12}$ is the sum of two positive terms one can safely assume that each $|(\Theta_L)_{N\mu}|^2$ and $|(\Theta_L)_{Ne}|^2 \sim 10^{-12}$ are individually smaller than 10^{-12} .

In what follows, we discuss how the above estimates translate to the sensitivity for the Dirac mass matrix elements $(M_D)_{eN}$ and $(M_D)_{\mu N}$ at the 100 TeV pp collider. To this end, it is instructive to show the relation between the Dirac mass matrix M_D and the heavy, light neutrino mass matrices when $|(V_L)_{ij}| = |(V_R)_{ij}|$, since in this case the relation is simple enough to be written in a compact analytic form for both \mathcal{C} and \mathcal{P} cases. From Eq (26) and for \mathcal{C} as the LR symmetry, the Dirac mass matrix M_D can be written as [15],

$$M_D = V_L^* \hat{M}_N \sqrt{\frac{v_L}{v_R} - \frac{\hat{M}_\nu}{\hat{M}_N}} V_L^\dagger. \quad (39)$$

Notice that this connection is lost for the non-minimal models, as can be explicitly seen in Eq. (33), since in this case there is an orthogonal, complex matrix \mathcal{R} which makes the Dirac mass arbitrary.

The same considerations apply also for \mathcal{P} as the LR symmetry where the Dirac mass matrix can be written as [16]

$$M_D = V_L \hat{M}_N \sqrt{\frac{v_L}{v_R} - \frac{\hat{M}_\nu}{\hat{M}_N}} V_L^\dagger \quad (40)$$

These results explicitly show that when CP is an exact symmetry, both LR symmetries coincide. When $|(V_L)_{i,j}| \neq |(V_R)_{i,j}|$, the relation between the Dirac mass matrix and the heavy and light neutrino mass matrices shown in Eqs. (39) and (40) is far more complicated, and this general situation has been discussed in Refs. [15–17]. Nevertheless, even in this general case, the connection still exists and can be found by solving numerically some algebraic equations.

In short, the results we found apply for both Parity and Charge-conjugation as the LR symmetry. In Fig. 10 (right panel), we plot, using Eqs. (39) and (40), the values for $(M_D)_{eN}$ and $(M_D)_{\mu N}$ in the same range of heavy neutrino masses. We can conclude that Dirac mass terms of the order of 10^{-1} MeV can be probed at the 100 TeV pp collider. In the case the results from the experiment does not match the predictions made by the minimal model, it would mean that the discrete LR symmetry must be explicitly broken in the Yukawa sector of the minimal model or that the LR symmetry is non-minimally realized.

Finally, it is interesting to observe that if approximate Parity symmetry is invoked as a solution to the Strong CP problem, the neutron electric dipole moment [63–66] constraint, together with the constraint coming from the indirect CP violation (ϵ_K) in the Kaon sector, would set $M_{W_R} \sim 20$ TeV [67]. This scale is the same scale that may be probed at the 100 TeV pp collider. Hence, the 100 TeV pp collider offers the unique opportunity of finding the W_R boson at the 20 TeV scale, probing the Yukawa sector of the minimal model and offering a solution to the Strong CP problem by invoking Parity as an approximate symmetry at higher energies [68].

5 Conclusions

In this work, we have analyzed the trilepton final state (produced via a W_R gauge boson) as an effective channel for probing the Dirac mass terms of neutrinos at hadronic colliders in the context of left-right symmetric models. We have assessed the sensitivity to the heavy-light mixing of heavy neutrinos at the LHC, the HE-LHC and a 100 TeV pp collider using the $pp \rightarrow W_R \rightarrow e^+ N \rightarrow e^+ (N \rightarrow e^+ W^- \rightarrow e^+ \mu^- \nu)$ channel. Within the minimal framework, the relation between the Dirac mass matrix in terms of the heavy and light neutrino mass matrices implies that it is possible to translate the sensitivity to the heavy-light neutrino mixing into a bound on the neutrino Dirac mass M_D . For instance, we found that the minimal framework would not be seen at the LHC and the HE-LHC in the purely leptonic decays even with the ultimate integrated luminosities. Equivalently, this means that if any positive signal in the purely leptonic channel with the kinematic features described here is seen at the LHC, one would conclude left-right symmetry must be realized in a non-minimal context.

Finally, for a 100 TeV pp collider with 30 ab^{-1} of integrated luminosity, we have found that for W_R boson masses between 6 – 20 TeV and heavy neutrinos masses between 80 – 460 GeV, the Dirac mass term $(M_D)_{eN}$ and $(M_D)_{\mu N}$ can be excluded at 2σ up to masses of the order of

10^{-1} MeV and when either parity or charge conjugation is the left-right symmetry. Furthermore, if the results of the experiment do not agree with the predictions given by the minimal model, the LR symmetry must be explicitly broken in the Yukawa sector or a non-minimal realization would be present.

Acknowledgements

J.V. thanks Goran Senjanović for illuminating discussions and useful suggestions during all the stages of this work. J.C.H. thanks Martin Hirsch for useful discussions. J.V., J.C.H. and N.N. are grateful to the UMass Amherst Center for Fundamental Interactions for the hospitality, where they were visitors during the initial stages of this work. J.V. was funded by FONDECYT grant No. 3170154 and by Conicyt PIA/Basal FB0821. J.C.H. is supported by Chile grants Fondecyt No. 1161463 and Conicyt PIA/ACT 1406. MJRM and H-L.L was supported in part under U.S. Department of Energy Contract DE-SC0011095. N.N. was supported by FONDECYT (Chile) grant 3170906. H-L.L is also supported by the National Science Foundation of China under Grants No. 11875003

References and Notes

- [1] J. C. Pati and A. Salam, *Lepton Number as the Fourth Color*, *Phys. Rev.* **D10** (1974) 275–289.
- [2] R. N. Mohapatra and J. C. Pati, *A Natural Left-Right Symmetry*, *Phys. Rev.* **D11** (1975) 2558.
- [3] G. Senjanović and R. N. Mohapatra, *Exact Left-Right Symmetry and Spontaneous Violation of Parity*, *Phys. Rev.* **D12** (1975) 1502.
- [4] G. Senjanović, *Spontaneous Breakdown of Parity in a Class of Gauge Theories*, *Nucl. Phys.* **B153** (1979) 334–364.
- [5] R. N. Mohapatra and G. Senjanović, *Neutrino Mass and Spontaneous Parity Violation*, *Phys. Rev. Lett.* **44** (1980) 912.
- [6] R. N. Mohapatra and G. Senjanović, *Neutrino Masses and Mixings in Gauge Models with Spontaneous Parity Violation*, *Phys. Rev.* **D23** (1981) 165.
- [7] ATLAS, CMS collaboration, G. Aad et al., *Combined Measurement of the Higgs Boson Mass in pp Collisions at $\sqrt{s} = 7$ and 8 TeV with the ATLAS and CMS Experiments*, *Phys. Rev. Lett.* **114** (2015) 191803, [1503.07589].

- [8] CMS collaboration, S. Chatrchyan et al., *Evidence for the direct decay of the 125 GeV Higgs boson to fermions*, *Nature Phys.* **10** (2014) 557–560, [1401.6527].
- [9] P. Minkowski, $\mu \rightarrow e\gamma$ at a Rate of One Out of 10^9 Muon Decays?, *Phys. Lett.* **67B** (1977) 421–428.
- [10] S. L. Glashow, *The Future of Elementary Particle Physics*, *NATO Sci. Ser. B* **61** (1980) 687.
- [11] M. Gell-Mann, P. Ramond and R. Slansky, *Complex Spinors and Unified Theories*, *Conf. Proc.* **C790927** (1979) 315–321, [1306.4669].
- [12] T. Yanagida, *HORIZONTAL SYMMETRY AND MASSES OF NEUTRINOS*, *Conf. Proc.* **C7902131** (1979) 95–99.
- [13] J. Schechter and J. W. F. Valle, *Neutrino Masses in $SU(2) \times U(1)$ Theories*, *Phys. Rev.* **D22** (1980) 2227.
- [14] W.-Y. Keung and G. Senjanović, *Majorana Neutrinos and the Production of the Right-handed Charged Gauge Boson*, *Phys. Rev. Lett.* **50** (1983) 1427.
- [15] M. Nemevsek, G. Senjanović and V. Tello, *Connecting Dirac and Majorana Neutrino Mass Matrices in the Minimal Left-Right Symmetric Model*, *Phys. Rev. Lett.* **110** (2013) 151802, [1211.2837].
- [16] G. Senjanović and V. Tello, *Probing Seesaw with Parity Restoration*, *Phys. Rev. Lett.* **119** (2017) 201803, [1612.05503].
- [17] G. Senjanovic and V. Tello, *Disentangling Seesaw in the Minimal Left-Right Symmetric Model*, 1812.03790.
- [18] J. A. Casas and A. Ibarra, *Oscillating neutrinos and muon $\rightarrow e, \gamma$* , *Nucl. Phys.* **B618** (2001) 171–204, [hep-ph/0103065].
- [19] A. Ferrari, J. Collot, M.-L. Andrieux, B. Belhorma, P. de Saintignon, J.-Y. Hostachy et al., *Sensitivity study for new gauge bosons and right-handed majorana neutrinos in pp collisions at $\sqrt{s} = 14\text{TeV}$* , *Phys. Rev. D* **62** (May, 2000) 013001.
- [20] T. Han, I. Lewis, R. Ruiz and Z.-g. Si, *Lepton Number Violation and W' Chiral Couplings at the LHC*, *Phys. Rev.* **D87** (2013) 035011, [1211.6447].
- [21] E. Izaguirre and B. Shuve, *Multilepton and Lepton Jet Probes of Sub-Weak-Scale Right-Handed Neutrinos*, *Phys. Rev.* **D91** (2015) 093010, [1504.02470].

- [22] CMS collaboration, A. M. Sirunyan et al., *Search for heavy neutral leptons in events with three charged leptons in proton-proton collisions at $\sqrt{s} = 13$ TeV*, *Phys. Rev. Lett.* **120** (2018) 221801, [1802.02965].
- [23] A. Das, N. Nagata and N. Okada, *Testing the 2-TeV Resonance with Trileptons*, *JHEP* **03** (2016) 049, [1601.05079].
- [24] J. Kersten and A. Yu. Smirnov, *Right-Handed Neutrinos at CERN LHC and the Mechanism of Neutrino Mass Generation*, *Phys. Rev.* **D76** (2007) 073005, [0705.3221].
- [25] A. de Gouvea, *GeV seesaw, accidentally small neutrino masses, and Higgs decays to neutrinos*, 0706.1732.
- [26] Z.-z. Xing, *Naturalness and Testability of TeV Seesaw Mechanisms*, *Prog. Theor. Phys. Suppl.* **180** (2009) 112–127, [0905.3903].
- [27] X.-G. He, S. Oh, J. Tandean and C.-C. Wen, *Large Mixing of Light and Heavy Neutrinos in Seesaw Models and the LHC*, *Phys. Rev.* **D80** (2009) 073012, [0907.1607].
- [28] A. Ibarra, E. Molinaro and S. T. Petcov, *TeV Scale See-Saw Mechanisms of Neutrino Mass Generation, the Majorana Nature of the Heavy Singlet Neutrinos and $(\beta\beta)_{0\nu}$ -Decay*, *JHEP* **09** (2010) 108, [1007.2378].
- [29] N. Haba, T. Horita, K. Kaneta and Y. Mimura, *TeV-scale seesaw with non-negligible left-right neutrino mixings*, 1110.2252.
- [30] M. Mitra, G. Senjanovic and F. Vissani, *Neutrinoless Double Beta Decay and Heavy Sterile Neutrinos*, *Nucl. Phys.* **B856** (2012) 26–73, [1108.0004].
- [31] C.-Y. Chen, P. S. B. Dev and R. N. Mohapatra, *Probing Heavy-Light Neutrino Mixing in Left-Right Seesaw Models at the LHC*, *Phys. Rev.* **D88** (2013) 033014, [1306.2342].
- [32] E. K. Akhmedov and M. Frigerio, *Interplay of type I and type II seesaw contributions to neutrino mass*, *JHEP* **01** (2007) 043, [hep-ph/0609046].
- [33] E. K. Akhmedov, M. Blennow, T. Hallgren, T. Konstandin and T. Ohlsson, *Stability and leptogenesis in the left-right symmetric seesaw mechanism*, *JHEP* **04** (2007) 022, [hep-ph/0612194].
- [34] W. Chao, S. Luo, Z.-z. Xing and S. Zhou, *A Compromise between Neutrino Masses and Collider Signatures in the Type-II Seesaw Model*, *Phys. Rev.* **D77** (2008) 016001, [0709.1069].

- [35] G. Senjanovi and V. Tello, *Right Handed Quark Mixing in Left-Right Symmetric Theory*, *Phys. Rev. Lett.* **114** (2015) 071801, [1408.3835].
- [36] G. Senjanovi and V. Tello, *Restoration of Parity and the Right-Handed Analog of the CKM Matrix*, *Phys. Rev.* **D94** (2016) 095023, [1502.05704].
- [37] S. Dube, D. Gadkari and A. M. Thalapillil, *Lepton-Jets and Low-Mass Sterile Neutrinos at Hadron Colliders*, *Phys. Rev.* **D96** (2017) 055031, [1707.00008].
- [38] V. Tello, *Connections between the high and low energy violation of Lepton and Flavor numbers in the minimal left-right symmetric model*. PhD thesis, SISSA, Trieste, 2012.
- [39] A. Maiezza, G. Senjanović and J. C. Vazquez, *Higgs sector of the minimal left-right symmetric theory*, *Phys. Rev.* **D95** (2017) 095004, [1612.09146].
- [40] M. K. Parida and A. Raychaudhuri, *Inverse see-saw, leptogenesis, observable proton decay and $\Delta_R^{\pm\pm}$ in SUSY $SO(10)$ with heavy W_R* , *Phys. Rev.* **D82** (2010) 093017, [1007.5085].
- [41] C. Arbelez, M. Hirsch, M. Malinsk and J. C. Romo, *LHC-scale left-right symmetry and unification*, *Phys. Rev.* **D89** (2014) 035002, [1311.3228].
- [42] R. N. Mohapatra and J. W. F. Valle, *Neutrino Mass and Baryon Number Nonconservation in Superstring Models*, *Phys. Rev.* **D34** (1986) 1642.
- [43] P. S. Bhupal Dev and R. N. Mohapatra, *Unified explanation of the $eejj$, diboson and dijet resonances at the LHC*, *Phys. Rev. Lett.* **115** (2015) 181803, [1508.02277].
- [44] G. Anamiati, M. Hirsch and E. Nardi, *Quasi-Dirac neutrinos at the LHC*, *JHEP* **10** (2016) 010, [1607.05641].
- [45] G. Anamiati, R. M. Fonseca and M. Hirsch, *Quasi Dirac neutrino oscillations*, *Phys. Rev.* **D97** (2018) 095008, [1710.06249].
- [46] M. Mitra, R. Ruiz, D. J. Scott and M. Spannowsky, *Neutrino Jets from High-Mass W_R Gauge Bosons in TeV-Scale Left-Right Symmetric Models*, *Phys. Rev.* **D94** (2016) 095016, [1607.03504].
- [47] M. Nemevsek, F. Nesti and G. Popara, *Keung-Senjanović process at LHC: from LNV to displaced vertices to invisible decays*, 1801.05813.
- [48] PARTICLE DATA GROUP collaboration, K. Nakamura et al., *Review of particle physics*, *J. Phys.* **G37** (2010) 075021.

- [49] C. Arbelaz, C. Dib, I. Schmidt and J. C. Vasquez, *Probing the Dirac or Majorana nature of the Heavy Neutrinos in pure leptonic decays at the LHC*, *Phys. Rev.* **D97** (2018) 055011, [1712.08704].
- [50] A. Alloul, N. D. Christensen, C. Degrande, C. Duhr and B. Fuks, *FeynRules 2.0 - A complete toolbox for tree-level phenomenology*, *Comput. Phys. Commun.* **185** (2014) 2250–2300, [1310.1921].
- [51] A. Roitgrund, G. Eilam and S. Bar-Shalom, *Implementation of the left-right symmetric model in FeynRules*, *Comput. Phys. Commun.* **203** (2016) 18–44, [1401.3345].
- [52] M. Nemevsek, F. Nesti and J. C. Vasquez, *Majorana Higgses at colliders*, *JHEP* **04** (2017) 114, [1612.06840].
- [53] J. Alwall, R. Frederix, S. Frixione, V. Hirschi, F. Maltoni, O. Mattelaer et al., *The automated computation of tree-level and next-to-leading order differential cross sections, and their matching to parton shower simulations*, *JHEP* **07** (2014) 079, [1405.0301].
- [54] T. Sjostrand, S. Mrenna and P. Z. Skands, *PYTHIA 6.4 Physics and Manual*, *JHEP* **05** (2006) 026, [hep-ph/0603175].
- [55] DELPHES 3 collaboration, J. de Favereau, C. Delaere, P. Demin, A. Giammanco, V. Lematre, A. Mertens et al., *DELPHES 3, A modular framework for fast simulation of a generic collider experiment*, *JHEP* **02** (2014) 057, [1307.6346].
- [56] ATLAS collaboration, M. Aaboud et al., *Search for doubly charged Higgs boson production in multi-lepton final states with the ATLAS detector using protonproton collisions at $\sqrt{s} = 13$ TeV*, *Eur. Phys. J.* **C78** (2018) 199, [1710.09748].
- [57] M. Nemevsek, F. Nesti, G. Senjanović and Y. Zhang, *First Limits on Left-Right Symmetry Scale from LHC Data*, *Phys. Rev.* **D83** (2011) 115014, [1103.1627].
- [58] J. C. Helo, M. Hirsch and S. Kovalenko, *Heavy neutrino searches at the LHC with displaced vertices*, *Phys. Rev.* **D89** (2014) 073005, [1312.2900].
- [59] G. Cottin, J. C. Helo and M. Hirsch, *Searches for light sterile neutrinos with multitrack displaced vertices*, *Phys. Rev.* **D97** (2018) 055025, [1801.02734].
- [60] G. Cottin, J. C. Helo and M. Hirsch, *Displaced vertices as probes of sterile neutrino mixing at the LHC*, *Phys. Rev.* **D98** (2018) 035012, [1806.05191].

- [61] A. Das, P. S. B. Dev and R. N. Mohapatra, *Same Sign versus Opposite Sign Dileptons as a Probe of Low Scale Seesaw Mechanisms*, *Phys. Rev.* **D97** (2018) 015018, [1709.06553].
- [62] M. L. Mangano et al., *Physics at a 100 TeV pp Collider: Standard Model Processes*, *CERN Yellow Report* (2017) 1–254, [1607.01831].
- [63] J. S. M. Ginges and V. V. Flambaum, *Violations of fundamental symmetries in atoms and tests of unification theories of elementary particles*, *Phys. Rept.* **397** (2004) 63–154, [physics/0309054].
- [64] M. Pospelov and A. Ritz, *Electric dipole moments as probes of new physics*, *Annals Phys.* **318** (2005) 119–169, [hep-ph/0504231].
- [65] T. Fukuyama, *Searching for New Physics beyond the Standard Model in Electric Dipole Moment*, *Int. J. Mod. Phys.* **A27** (2012) 1230015, [1201.4252].
- [66] J. Engel, M. J. Ramsey-Musolf and U. van Kolck, *Electric Dipole Moments of Nucleons, Nuclei, and Atoms: The Standard Model and Beyond*, *Prog. Part. Nucl. Phys.* **71** (2013) 21–74, [1303.2371].
- [67] A. Maiezza and M. Nemevsek, *Strong P invariance, neutron electric dipole moment, and minimal left-right parity at LHC*, *Phys. Rev.* **D90** (2014) 095002, [1407.3678].
- [68] R. N. Mohapatra and G. Senjanović, *Natural Suppression of Strong p and t Noninvariance*, *Phys. Lett.* **79B** (1978) 283–286.